



Published in final edited form as:

Mucosal Immunol. 2015 January ; 8(1): 141–151. doi:10.1038/mi.2014.51.

Unique Lamina Propria Stromal Cells Imprint the Functional Phenotype of Mucosal Dendritic Cells

Ildefonso Vicente-Suarez¹, Alexandre Larange¹, Colin Reardon¹, Michael Matho², Sonia Feau¹, Grzegorz Chodaczek¹, Yunji Park^{1,3}, Yuuki Obata^{4,5}, Rebecca Gold¹, Yiran Wang-Zhu¹, Chris Lena¹, Dirk M. Zajonc², Stephen Schoenberger¹, Mitchell Kronenberg¹, and Hilde Cheroutre¹

¹Division of Developmental Immunology, La Jolla Institute for Allergy and Immunology, La Jolla CA 92037, USA

²Division of Cell Biology, La Jolla Institute for Allergy and Immunology, La Jolla CA 92037, USA

³Division of Integrative Biosciences and Biotechnology, Pohang University of Science and Technology, Pohang, Korea

⁴Division of Mucosal Barriology, International Research and Development Center for Mucosal Vaccines, The Institute of Medical Science, The University of Tokyo, Tokyo 108-8639, Japan

⁵Laboratory for immune regulation, Graduate School of Medicine, Chiba University, Chiba 260-8670, Japan

Abstract

Mucosal dendritic cells (DCs) in the intestine acquire the unique capacity to produce retinoic acid (RA), a vitamin A metabolite that induces gut tropism and regulates the functional differentiation of the T cells they prime. Here we identified a stromal cell (SC) population in the intestinal lamina propria (LP), which is capable of inducing RA production in DCs in a RA- and granulocyte-macrophage colony-stimulating factor (GM-CSF)-dependent fashion. Unlike DCs, LP SCs constitutively expressed the enzymatic machinery to produce RA even in the absence of dietary vitamin A but were not able to do so in germ-free mice implying regulation by microbiota. Interestingly, DCs promoted GM-CSF production by the SCs indicating a two-way crosstalk between both cell types. Furthermore, RA-producing LP SCs and intestinal DCs localized closely *in vivo* suggesting that the interactions between both cell types might play an important role on the functional education of migratory DCs and therefore in the regulation of immune responses towards oral and commensal antigens.

Users may view, print, copy, and download text and data-mine the content in such documents, for the purposes of academic research, subject always to the full Conditions of use:http://www.nature.com/authors/editorial_policies/license.html#terms

Correspondence and requests for materials should be addressed to H.C. (hilde@liai.org).

Description of the individual contribution made by each author

I.V.S designed and performed experiments, analyzed data and contributed in the writing of the manuscript. A.L and C.R performed experiments, discussed the results and implications and edited the manuscript. M.M, S.F and Y.O performed experiments and analyzed results. R.G performed experiments. Y.W and C.L provided technical assistance. S.P.S, D.Z and M.K gave conceptual advice. H.C designed experiments, discussed the results and their implications, supervised the experiments and wrote the manuscript.

Competing Interests statement. The authors declare no competing financial interests.

Introduction

Genetic regulation by vitamin A is involved in multiple biological processes such as embryonic development, vision and immunity¹. To exert this regulatory role, vitamin A is oxidized into its active form by retinol dehydrogenases (RDH) followed by retinal dehydrogenases (RALDH)². The product of this metabolism, retinoic acid (RA), binds to nuclear RA receptors (RARs), and together drive the transcription of target genes that contain RA responsive elements (RARE) within their promoters³.

RA is especially critical for the regulation of immune responses within the digestive tract, thereby controlling functional T cell differentiation and directing lymphocyte migration towards the intestine^{4,5}. Accordingly, dendritic cells (DCs) in the lamina propria (LP), Peyer's patches (PPs) and mesenteric lymph nodes (MLNs) but not spleen- or peripheral lymph nodes express RALDH and produce RA⁴. Under steady-state conditions RA contributes to dampening effector responses by blocking Th1 and Th17 differentiation and enhancing IgA production as well as TGF β -driven Treg differentiation⁵⁻⁸. In contrast, under inflammatory conditions, in the presence of IL-15, RA exacerbates immune pathology by driving IL-12 production⁹. These observations place RA as a master regulator of tolerogenic as well as inflammatory immune responses especially in the digestive tract.

CD103-expressing migratory DCs that transport and present gut-derived antigens to naive T cells in the MLNs typically produce RA^{10,11}, suggesting that they gain this hallmark feature during their education and maturation in the intestinal compartment. In agreement with this notion, MLNs of mice deficient for the chemokine receptor 7 (CCR7), which is required for efficient lymph node homing, are lacking mucosal RA-producing DCs¹¹.

Despite this, it is not known how migratory DCs acquire RALDH activity, and the relevance of different factors such as cytokines or the presence of commensals has been alternatively supported or rejected by different studies^{12,13}. Nonetheless, there is substantial evidence demonstrating that RA signaling is required and might be sufficient for the initial induction of RALDH in DCs, not in the least the observation that vitamin A deficient (VAD) mice lack RALDH⁺ DCs in the LP and MLNs^{14,15} and that exposure to exogenous RA was sufficient to induce RALDH activity in DCs as shown in some reports^{16,17}.

To identify *in vivo* the intestinal cell type that has the capacity to educate migratory DCs and to elucidate the mechanisms that lead to RA production by CD103⁺ DCs, we dissected and characterized various cell subsets from the intestinal LP and identified a stromal cell population capable of imprinting DCs with RALDH activity. These stromal cells (SCs) are an abundant component of the intestinal LP and might represent a direct source of RA. Importantly, we show that these SCs are in close contact with CD103-expressing DCs and that this interaction conversely promotes GM-CSF secretion by the SCs, which in addition to RA, is absolutely required for effective RALDH induction in the DC compartment. Finally, we also found that unlike DCs, the constitutive RALDH expression by LP SCs is independent of RA whereas it did require the presence of the microbiota. Our findings therefore identified an RA-producing LP SC as a direct sensor of the gut environment and an important regulator of the functional maturation of mucosal DCs. The results also

demonstrate an unexpected two-way crosstalk between these SCs and the DCs that might play an important role in controlling the tolerogenic or inflammatory nature of the mucosal immune response.

Results

A subset of intestinal lamina propria stromal cells produce RA

Mucosal migratory DCs are marked by the expression of RALDH and the capacity to produce RA, which modulates the immune response^{4,5,6}. RA is required to induce RALDH expression in mucosal DCs suggesting that they might be initially exposed to RA during their development in the LP¹⁴. Nevertheless, the source of RA as well as the education process that grants mucosal DCs their unique immune regulatory capacity are still poorly understood. To identify potential local sources of RA, we analyzed LP cells using aldefluor, a fluorescent RALDH substrate that marks those cells with the capacity to produce RA. Interestingly, a significant population of CD45-negative cells displayed high RALDH activity (Figure 1a **upper left panel**). The majority of these RALDH positive cells were negative for the epithelial cell marker Epcam (CD326) (Figure 1a **upper right panel**) suggesting that in addition to intestinal epithelial cells (IECs), which are known to constitutively express RALDH^{4,18,19} there is a subset of cells in the LP that also produces RA. RALDH activity among the SCs was confined to a specific population that shows remarkable similarities with the well-characterized fibroblastic reticular cells (FRCs). These similarities included the expression of podoplanin (Pdpn) in the absence of, CD31 (Figure 1a **lower left panel**) and they expressed ICAM-1 alone or in combination with VCAM-1 (Figure 1a **lower right panel**). RALDH expression in sorted CD31⁻ CD45⁻ Epcam⁻ Pdpn^{hi} small intestinal (SI) LP SCs was confirmed by qPCR. Unlike IECs, which mainly expressed *aldh1a1*, Pdpn⁺CD31⁻ SCs expressed high levels of all three RALDH encoding genes, *aldh1a1*, -2 and -3 (Figure 1b). To assess if aldefluor positive SCs also produced RA, supernatants from overnight cultures of these cells were used to stimulate a reporter cell line that produces β -galactosidase under the control of an RA responsive element (RARE)²⁰. In agreement with active secretion of RA, supernatants increased β -galactosidase production relative to media as measured through a colorimetric reaction (Figure 1c **left panel**), and the absorbance values obtained were similar to those of media supplemented with 4 nM RA (Figure 1c **right panel**).

To test if ALDH expression by Pdpn⁺CD31⁻ SCs was RA dependent, we compared aldefluor staining in LP cells isolated from Vitamin A-deficient (VAD) and -sufficient (VAS) mice (Figure 1d). We did not find a significant difference between both conditions suggesting that, in contrast to migratory DCs^{14,15} (Supplementary Figure S1), RA was not required for the induction or maintenance of the RA metabolism machinery in LP SCs. Interestingly, RALDH expression in the LP SCs, but not in the DCs, did depend on the presence of the intestinal microbiota as aldefluor staining was practically undetectable in SCs from germ free mice (Fig 1e and Supplementary Figure S1).

RALDH⁺ LP SCs directly interact with CD103⁺DCs *in vivo*

To investigate the location of RALDH positive SCs within the LP compartment, aldefluor staining was directly performed in live SI explants in which the epithelial layer was removed to allow penetration of the reagent into the intestinal mucosa. Aldefluor bright cells were numerous and distinct from the CD31⁺ endothelial cells and platelets, which marked the blood vessels in the villi (Figure 2a). In order to examine the proximity of these RA-producing SCs to DCs in the LP, we co-stained tissue explants with aldefluor and the DC marker, CD11c. Aldefluor bright SCs were clearly noticeable in the vicinity of the CD11c⁺ cells but not in the presence of the RALDH inhibitor DEAB indicating that the fluorescence observed correlated with RALDH activity (Figure 2b). More importantly, merged staining of CD11c and aldefluor at the interface between RA-producing SCs and CD11c⁺ cells indicated that there was direct contact between the two cell types (Figure 2c).

Remarkably, many of the CD11c⁺ cells that directly contacted the aldefluor bright SCs were also dim for aldefluor staining (Figure 2c). CD11c expression is not exclusive for DCs but co-staining of CD11c together with CD103 faithfully identifies migratory DCs^{10,11}. Contact between aldefluor bright stromal cells and CD11c⁺ cells that co-stained for CD103 was particularly striking, suggesting that *in vivo* there is a direct crosstalk between RA producing LP SCs and migratory DCs that acquire the regulatory capacity to produce RA (Fig 2c).

RALDH⁺ LP SCs induce RALDH activity in splenic DCs

To test if aldefluor⁺ LP SCs have the capacity to induce RA production in DCs, we sorted SI Pdpn⁺ CD31⁻ SCs and co-cultured them for 24h with splenic DCs. After conditioning with Pdpn⁺ CD31⁻ SCs, splenic DCs became aldefluor high (Figure 3A). Furthermore, compared to unconditioned DCs, SCs-cocultured DCs suppressed Th17 differentiation and induced the gut homing receptors $\alpha 4\beta 7$ and CCR9 (Figure 3B and Supplementary Figure S2a), both typical effects of RA^{4,6}.

The effects were blocked when the RALDH inhibitor DEAB was added, ruling out that they were caused by a carryover of RA from the SCs-coculture, since active production of the metabolite by RALDH in the DCs was required (Figure 3B). Surprisingly, SCs-cocultured DCs did not significantly increase TGF- β mediated Foxp3⁺Treg differentiation⁶ *in vitro* (Supplementary Figure S2b, **upper panels**). However, because SCs-conditioned DCs showed signs of activation as indicated by the increased expression of activation markers including, CD86 (Supplementary Figure S2c), it is likely that Foxp3⁺Treg differentiation is suppressed under these co-culture conditions⁸. In support of this, when RA production by the DCs was blocked with DEAB, SCs-conditioned DCs induced much less Foxp3⁺Treg differentiation compared to untreated DCs (Supplementary Figure S2b, **lower panels**), indicating that RA produced by the activated SCs-conditioned DCs did enhance the Foxp3⁺Treg differentiation. Interestingly, when RA production was blocked, SCs-conditioned DCs induced more Th17 differentiation than untreated DCs (Figure 3b **SCs cond.+DEAB**) suggesting that the LP SCs also enhanced the functional priming capacity of the DCs they interacted with.

To investigate if soluble factors released by Pdpn⁺ CD31⁻ SCs were able to educate DCs, we conditioned splenic DCs for 24h with media harvested from Pdpn⁺ CD31⁻ SCs overnight cultures. Splenic DCs stimulated with these supernatants specifically upregulated *aldh1a2* expression (Figure 3C), which is the RALDH isoform typically expressed by the mucosal migratory DCs.

Furthermore a global RAR antagonist (BMS 204493) blocked RALDH expression in DCs induced either by direct contact with Pdpn⁺ CD31⁻ SCs (Figure 3d, **left panel**) or by SCs-derived supernatants (Figure 3d, **right panel**), indicating that RALDH induction in DCs depended on RA signaling. Overall, these data demonstrate that LP Pdpn⁺ CD31⁻ SCs can induce RA-dependent transcriptional activation of *aldh1a2* in DCs, which leads to the expression of RALDH2 and the production of RA, a hallmark feature of the migratory mucosal CD103⁺ DC.

GM-CSF produced by the LP SCs is required for the RA-induced RALDH expression in DCs

To investigate if RA secreted by the SCs is sufficient to induce RALDH expression in spleen DCs, various concentrations of RA were added to overnight cultures of spleen DCs. Unlike supernatants from the RALDH⁺ LP SCs, RA by itself was inefficient to induce RALDH expression in the overnight cultured DCs (Figure 4a). In contrast, RA added to spleen DCs co-cultured with a RALDH⁻ CD45⁻ Pdpn^{hi} spleen stromal cell line markedly increased aldefluor staining in the DCs, comparable to the level induced by the RALDH⁺ LP SC (Figure 4b, **left and middle panels**). These data indicated that the spleen and LP SCs produced one or more factors that synergize with RA to mediate the expression of RALDH in co-cultured DCs. To identify the nature of this stromal cell-derived factor, supernatants from the aforementioned spleen SC cell line were concentrated and digested or not with proteinase K, and used to condition spleen DCs in the presence of exogenous RA. Proteinase digestion completely abrogated the induction of RALDH in the DCs, indicating that the factor(s) secreted by the SCs were of a protein nature (Figure 4b, **right panel**). To characterize the protein(s), we tested various size fractions of the supernatants for their ability to synergize with exogenous RA to induce RALDH expression in spleen DCs. Biological activity was detected in size fractions around 30 kD (Figure 4c). The molecular size range corresponds to the size of GM-CSF, which was shown before to also be a potent inducer of RALDH in DCs¹⁵. To test if the factor released by the SCs was indeed GM-CSF, conditioned spleen DCs co-cultured with either LP SCs isolated from GM-CSF^{-/-} animals or WT LP SCs and anti-GM-CSF blocking antibodies, were analyzed for RALDH induction. In the absence of GM-CSF, RALDH expression in the cocultured DCs was clearly impaired, indicating that GM-CSF produced by the SCs played a critical role in the RA-dependent transcriptional activation of *aldh1a2* in DCs (Figure 4d). In order to confirm that RA signaling was required to induce RALDH2 expression in DCs, even in the presence of GM-CSF, we cultured DCs with GM-CSF in serum free media, since serum can be a source of retinoids²¹. GM-CSF alone was inefficient to support the induction of RALDH2 in cultured DCs, whereas the addition of RA greatly enhanced aldefluor staining, further supporting the existence of synergy between GM-CSF and RA in DC imprinting (Supplementary Figure S3).

To address the relative importance of the direct contact observed *in vivo* between the CD103⁺DCs and the RA and GM-CSF producing LP SCs, spleen DCs and Pdpn⁺CD31⁻ LP SCs were cocultured either together in the same well or separated by a permeable membrane (transwell). Although, some RALDH imprinting was observed in DCs cultured under transwell conditions, the RALDH induction was much more powerful when spleen DCs were in direct contact with the SCs in the same well (Figure 4e). Interestingly, GM-CSF production by the SCs was markedly increased in these cocultures as compared to SCs cultured alone, implying that direct contact between the DCs and SCs conversely increases the ability of these SCs to produce GM-CSF (Figure 4f).

In summary, the data show that RA and GM-CSF produced by LP SCs synergize to imprint DCs with the ability to produce RA and to functionally mature. Furthermore, the *in vivo* observation indicating a direct contact between RALDH⁺ LP SCs and CD103⁺ DC, together with the finding that this interaction regulates GM-CSF production by the SCs, suggest that a direct crosstalk between these two cell types is required to ensure local imprinting of mucosal migratory DCs, which directs tolerogenic and inflammatory immune responses in the intestine.

The generation of CD11b⁺CD103⁺ DCs and their capacity to produce RA are uniquely impaired in the absence of GM-CSF

To address the *in vivo* relevance of GM-CSF for the acquisition of the RA producing capacity by SI LP DCs, we analyzed GM-CSF deficient mice. GM-CSF is known to contribute to the survival of tissue-resident DCs²² and in agreement, we detected a dramatic reduction of the SI LP CD11b⁺ CD103⁺ DC population (Figure 5a). Surprisingly, however, CD11b⁻CD103⁺ DCs were not affected and even increased in the absence of GM-CSF (Figure 5a). In addition, whereas the few remaining CD103⁺ CD11b⁺ DC showed impaired capacity to produce RA in the absence of GM-CSF, this capacity was not reduced in the CD11b⁻ CD103⁺ population (Figure 5b). These findings indicate that the LP SC-crosstalk might uniquely control the generation and/or survival and functional capacity of the SI migratory CD103⁺CD11b⁺ DC subset.

Discussion

The data presented here identify a type of LP SCs as a new player in mucosal immune regulation, able to interact with local DCs and rendering them capable to produce RA. These SCs expressed cell surface markers typical of FRCs, including ICAM-1, VCAM-1 and Pdpn^{23,24}, known to interact with integrins such as CD11b expressed by DCs. This interaction was directly demonstrated *in vivo* using confocal microscopy and provides strong support for a close communication between these two cell types *in situ*. More importantly, these SCs expressed high levels of the *aldh1a1*, *aldh1a2* and *aldh1a3* isozymes, indicating that they were capable of producing RA. Interestingly, Pdpn⁺ SCs from MLNs but not PLNs are also capable of expressing RALDH enzymes and promoting the induction of gut homing receptors on T cells^{25,26}. *In vivo* though, it is unlikely that these MLN SCs directly contribute to the RA-dependent imprinting of the intestinal migratory DCs, which occurs locally¹¹. Nevertheless, it is still possible that MLNs SCs imprint local resident DCs in the

LN or provide RA directly to T cells during priming. Further investigation is needed to fully understand the role of these RA-producing MLN SCs.

Intestinal LP SCs, unlike DCs^{14,15} expressed RALDH enzymes constitutively and independently of Vitamin A, suggesting that these SCs might serve as a primary source of RA for the initial education and imprinting of the RA processing machinery in migratory DC precursor cells. In support of this, splenic DCs cultured overnight with Pdpn⁺CD31⁻ intestinal SCs upregulated *aldh1a2* expression and gained other features associated with intestinal mucosal DCs. While independent of Vitamin A, SCs depended on the microbiota for their educational activity and failed to produce RA in germ free mice.

Gut epithelial cells also have the capacity to produce RA^{18,19} and RA-controlled gene transcription plays an important part of the epithelial cell differentiation and maturation. Furthermore *in vitro* studies²⁷ showed that human IECs could imprint co-cultured DCs through RA together with TGF β . DCs within the LP separated by the basal membrane from the epithelium makes it unlikely that imprinting by IECs contributes significantly to the education of migratory DCs *in vivo*.

Secreted RA alone is sufficient to induce RALDH2 expression in DCs^{16,17} however the drastic increase in enzyme expression in DCs cocultured with LP SCs indicated that additional factors and/or direct contact between the two cell types further promoted the functional education of the DCs. In support of this notion, we identified GM-CSF produced by LP SCs, as an important cofactor in this education. Nevertheless, the role of GM-CSF in the functional imprinting of mucosal DCs has been controversial^{15,28}. Our data here show a significant loss of the CD11b⁺CD103⁺ DC subset in the absence of GM-CSF whereas CD11b⁻CD103⁺ DCs are increased. As a result, the total number of CD11c⁺CD103⁺DCs did not change in GM-CSF deficient conditions as compared to WT mice. However, the few remaining CD11b⁺CD103⁺ DCs in the GM-CSF^{-/-} animals, showed impaired capacity to produce RA, whereas the increased subset of CD11b⁻CD103⁺DCs showed no defect. Therefore, when all CD11c⁺ CD103⁺ cells of GM-CSF KO animals are analyzed as one pool, no noteworthy impairment in the capacity to produce RA can be detected. In contrast, when the CD11b⁺ CD103⁺ subset is analyzed separately, a significant defect is evident, suggesting that GM-CSF is required for the generation and/or survival²² and imprinting of the CD11b⁺CD103⁺ DC subset, whereas GM-CSF is not required for the development or the imprinting of the CD11b⁻CD103⁺ DCs. The unique effect of GM-CSF produced by the LP SCs to control the generation and education of the SI CD103⁺CD11b⁺ DC subset but not the CD103⁺CD11b⁻ DC indicate that different SI LP DC populations might be educated through different mechanisms. This model could also explain the presence of SI LP CD103⁺DCs with RA producing capacity observed in GF mice even when this capacity was impaired in LP SCs. It is possible that SC-derived GM-CSF plays a role in the induction of the transcription factor IRF4, which is uniquely required for the development and function of the SI migratory CD103⁺CD11b⁺ DC subset²⁹.

GM-CSF, together with RA, is also absolutely required for the education of fully differentiated DCs, indicating that GM-CSF might be necessary to sensitize mature DCs, recruited to the LP from elsewhere, to RA imprinting. Interestingly, GM-CSF production by

the SCs was significantly increased when fully differentiated DCs were added to the culture, suggesting that a direct two-way crosstalk initiates and promotes the unique functional education of DCs that are in close proximity of the LP stromal cells. This has important implications, not only for the education of local mucosal migratory DC at steady state but also for the re-education of newly recruited peripheral or BM-derived mature DCs that migrate to the intestine in response to an inflammatory trigger. The result of SCs-mediated imprinting and functional education might ameliorate or exacerbate inflammation as RA in combination with regulatory cytokines such as TGF- β or inflammatory cytokines such as IL-15, can either promote tolerance and the generation of Foxp3 Tregs or potentiate the inflammatory immune response by generating pathogenic CD8 $\alpha\beta$ and CD4 effector cells⁹. Furthermore, the unique effect of GM-CSF, to selectively affect the generation and function of the CD103⁺CD11b⁺ DC subset, could also suggest an important role for the SI LP SCs in controlling the IRF4-dependent, IL-6 production by the CD11b⁺ DCs important for the intestinal Th17 cell differentiation^{29,30}. Therefore, the SCs identified here, might be key players in directing and controlling the immune response at the mucosal forefront. The fact that the SCs depend on the presence of the microflora for their educational role, further suggests that they are important sentinels that have the capacity to report on the condition of the intestinal lumen and accordingly regulate the tolerogenic or inflammatory nature of the immune response.

Methods

Mice

C57BL/6 and OT-II TCR-transgenic were purchased from The Jackson Laboratories (USA). GM-CSF knock-out mice were generously provided by Dr Whitsett (Cincinnati Children's Research Foundation). Mice were maintained under specific pathogen-free conditions at the La Jolla Institute for Allergy and Immunology vivarium. Animal care and experimentation were consistent with the NIH guidelines and were approved by the Institutional Animal Care and Use Committee at the La Jolla Institute for Allergy and Immunology. Swiss Webster germ free mice and age gender matched controls were purchased from Taconics.

Generation of vitamin A deficient mice

To generate vitamin A-deficient mice (VAD), pregnant females received either a chemically defined diet that lacked vitamin A (AIN-93M) or control diet containing retinyl acetate (25,000 IU/kg) (Dyets, USA). VAD diet started at 7–10 days of gestation and the pups were weaned at 3 weeks of age and maintained on the same diet at least until 11 weeks of age before analysis were performed.

Epithelial cell removal and single cell preparation from intestinal LP

To obtain LP stromal cells and DCs, small intestines were removed, washed and cut into 2–3 inches pieces. To remove the epithelial layer these pieces were placed in HBSS 5% FBS 0.5 M EDTA and shaken at 250 rpm for 5 minutes at 37°C and vortex for 1 min at room temperature, the tissue pieces were recovered using a stainless steel sieve, the buffer discarded and this process was repeated three times. The remaining intestinal tissue was minced and digested using collagenase type IV (Sigma Aldrich) for 20 minutes at 37°C.

Released cells were pelleted by centrifugation, washed with HBSS 5% FBS and passed through a 70 μm . These cells were stained for the markers Epcam, CD45, Podoplanin and CD31 for stromal cell sorting and CD45, MHCII, CD11c, CD11b and CD103 for DC sorting.

Analysis of RALDH activity by aldefluor staining

RALDH activity in individual cells was analyzed using the aldefluor staining kit (StemCell Technologies, Canada). Briefly, 1×10^6 cells were resuspended in the kit Assay Buffer containing activated aldefluor substrate (150 nM) and incubated for 30 min at 37 °C in the presence or absence of the RALDH inhibitor DEAB (100 μM). Afterwards cells were washed, placed on ice and stained for surface markers.

Real Time PCR

Total RNA was extracted using TriZol reagent (Qiagen, Valencia, CA), and cDNA obtained with the iScript cDNA synthesis kit (Bio-Rad, Hercules, CA). Target mRNA was quantified using SYBR green (Roche) and gene expression normalized relative to GAPDH. Data was collected and analyzed on a LightCycler 380 (Roche). Primers used were GAPDH fwd ATGGCCTTCCGTGTTCCCTAC, GAPDH rev AGATGCCTGCTTACCAC, Aldh1a1 fwd TGTGGGAATACCGTGGTTGTC, Aldh1a1 rev GTGAAGAGCCGTGAGAGGAG, Aldh1a2 fwd GTGGGAGAGTGTTCCTGTCT, Aldh1a2 rev TGCCTTGTCTATATCCACCTTGT, Aldh1a3 fwd GAGCAGCAATTCCTCCCATC, Aldh1a3 rev GAGCCGGTGAAGGCTATCT, Rara fwd TCCGAAGAGATAGTACCAGC, Rara rev AAAGCAAGGCTTGTAGATGCG, Rarb fwd AAGTGCTTTGAAGTGGGCAT, Rarb rev CTCTGTGCATTCTGCTTTG Rarg fwd AAGTACACCACGAACTCCAGT, Rarg rev TTCGCAAACCTCCACAATCTTGA

In vitro T cell stimulation with DCs

Splenic DCs were obtained by collagenase type IV digestion (Sigma Aldrich) (1 mg/ml) plus DNase I 40 U/ml (Roche) and the single cell suspension enriched using anti-CD11c beads and MACS columns (Miltenyi Biotec, USA), for some experiments cell were afterwards sorted as CD11c⁺MHCII^{hi} cells. When DCs were cocultured with SCs, CD45⁻Epcam⁻Podoplanin⁺CD31⁻ cells were sorted the day before the splenic DC preparation and cultured overnight in IMDM media supplemented with 10% FCS, 55 μM 2-Mercaptoethanol (Life Technologies-Gibco, NY) and antibiotics (Antibiotic-Antimycotic, Gibco, NY)(density 25×10^3 cells per well in a 96 well plate flat bottom). After overnight cultured basically all cells sorted are attached to the plate and display a fibroblast-like appearance. DCs are co-cultured with SCs for 24h. At this time DCs were harvested from the coculture by gently washing the wells, a procedure that released the majority of DCs while the stromal cells remained attached to the plate. OTII cells were isolated as in⁶ DCs and T cells were plated following a 1: 5 ratio (1×10^4 DCs : 5×10^4 OTII) and OVA peptide (1 μM) plus the indicated cytokines β (5 ng/ml), IL-6 (20 ng/ml) were added to the media. After 4–5 days of culture T cells were harvested, washed and expression of surface markers and cytokines assessed by flow cytometry. Briefly cells were incubated for 4–5h with 50 ng/ml PMA, 750 ng/ml Ionomycin (both Sigma, USA) and 10 $\mu\text{g/ml}$ Brefeldin A (Invitrogen, USA) in a tissue culture incubator at 37°C. After surface staining, cells were

resuspended in Fixation/Permeabilization solution (BD Cytotfix/Cytoperm kit-BD, USA), and intracellular cytokine staining performed according to the protocol in this kit.

Immunofluorescence staining

For in situ aldefluor staining intestinal explants were washed 3 times in HBSS 5% FBS 0.5M EDTA for 10 min at 37°C and shaking at 250 rpm in order to remove the epithelial layer. Afterwards, tissues were incubated in aldefluor assay buffer together with aldefluor reagent (1.5 μM) in the presence or absence of the RALDH inhibitor DEAB (100 μM). After that, tissues were washed, placed on ice and stained for surface markers.

RA measurement using F9-RARE-lacZ reporter cell line

Sorted CD45⁻Epcam⁻Podoplanin⁺CD31⁻ cells were cultured overnight in IMDM media supplemented with 10% FCS, 55μM 2-Mercaptoethanol (Life Technologies-Gibco, NY) and antibiotics (Antibiotic-Antimycotic, Gibco, NY)(density 25×10³ cells per well in a 96 well plate flat bottom). Supernatants were stored at -80C and measurement of retinoids performed as in^{3,31}. Briefly, F9-RARE-lacZ reporter cell line cells were grown in gelatinized flasks in DMEM media supplemented with 15% FBS and 0.8 mg/ml geneticin (G418) media. Once cells were near confluency they were detached from the flask using trypsin/EDTA (Gibco, NY). Cells were washed and resuspended at 2 million cells/ml density and plated in a flat bottom 96 well tissue culture plate at 2 × 10⁵ cells per well (100 microliters from initial dilution) plus 100 microliters media, different concentrations of RA or cell supernatants. After overnight culture, supernatants were removed and cells washed extensively with ice cold PBS. Following, cells were lysed and β-galactosidase activity assayed using the β-galactosidase enzyme assay system with reporter lysis buffer from Promega. Values obtained from known RA concentrations were used to draw a standard curve to quantify RA levels on the cell supernatants.

Supernatant fractionation

Supernatants were subjected to anion exchange chromatography (AEC, GE Healthcare, MonoQ 5/50 GL, cat #17-5166-01) and 1 ml fractions were collected along an increasing gradient of sodium chloride (0–1M). Fractions were used to treat DCs (50 microliters per well in a 96 well plate, total volume per well 200 microliters) and the fraction that stimulated the highest RALDH2 upregulation subjected to size exclusion chromatography (SEC), 0.5ml fractions were collected and used as before to stimulate DCs.

Supplementary Material

Refer to Web version on PubMed Central for supplementary material.

Acknowledgments

We wish to thank Dr Noelle for providing us with the F9 RARE lacZ cell line, Dr Whitsett for the GM-CSF knock-out mice and Dr Buckley for the Pdpn^{hi} splenic stromal cell line and C Kim and K v Gunst for cell sorting and M Cheroutre for her contribution. This work was supported by NIH R01 grants: R01AI050265 and DP1OD006433.

References

1. Mark M, Ghyselinck NB, Chambon P. Function of retinoid nuclear receptors: lessons from genetic and pharmacological dissections of the retinoic acid signaling pathway during mouse embryogenesis. *Annu Rev Pharmacol Toxicol.* 2006; 46:451–480. [PubMed: 16402912]
2. Napoli J. Interactions of retinoid binding proteins and enzymes in retinoid metabolism. *Biochimica et Biophysica Acta (BBA) - Molecular and Cell Biology of Lipids.* 1999; 1440:139–162. [PubMed: 10521699]
3. Petkovich M. Regulation of gene expression by vitamin A: the role of nuclear retinoic acid receptors. *Annu Rev Nutr.* 1992; 12:443–471. [PubMed: 1323983]
4. Iwata M. Retinoic Acid Imprints Gut-Homing Specificity on T Cells. *Immunity.* 2004; 21:527–538. [PubMed: 15485630]
5. Mora JR, et al. Generation of gut-homing IgA-secreting B cells by intestinal dendritic cells. *Science (New York, N.Y.).* 2006; 314:1157–1160.
6. Mucida D, et al. Reciprocal TH17 and regulatory T cell differentiation mediated by retinoic acid. *Science (New York, N.Y.).* 2007; 317:256–260.
7. Coombes J, et al. A functionally specialized population of mucosal CD103+ DCs induces Foxp3+ regulatory T cells via a TGF-beta and retinoic acid-dependent mechanism. *The Journal of Experimental Medicine.* 2007; 204:1757–1764. [PubMed: 17620361]
8. Benson MJ, Pino-Lagos K, Roseblatt M, Noelle RJ. All-trans retinoic acid mediates enhanced T reg cell growth, differentiation, and gut homing in the face of high levels of co-stimulation. *J Exp Med.* 2007; 204:1765–1774. [PubMed: 17620363]
9. DePaolo RW, et al. Co-adjuvant effects of retinoic acid and IL-15 induce inflammatory immunity to dietary antigens. *Nature.* 2011; 471:220–224. [PubMed: 21307853]
10. Jaensson E, et al. Small intestinal CD103+ dendritic cells display unique functional properties that are conserved between mice and humans. *J. Exp. Med.* 2008
11. Johansson-Lindbom B, et al. Functional specialization of gut CD103+ dendritic cells in the regulation of tissue-selective T cell homing. *J. Exp. Med.* 2005; 202:1063–1073. [PubMed: 16216890]
12. Agace W, Persson E. How vitamin A metabolizing dendritic cells are generated in the gut mucosa. *Trends in Immunology.* 2012; 33:42–48. doi: [PubMed: 22079120]
13. Cassani B, Villablanca E, De Calisto J, Wang S, Mora R. Vitamin A and immune regulation: Role of retinoic acid in gut-associated dendritic cell education, immune protection and tolerance. *Molecular Aspects of Medicine.* 2012; 33:63–76. doi: [PubMed: 22120429]
14. Molenaar R, et al. Expression of Retinaldehyde Dehydrogenase Enzymes in Mucosal Dendritic Cells and Gut-Draining Lymph Node Stromal Cells Is Controlled by Dietary Vitamin A. *The Journal of Immunology.* 2011; 186:1934–1942. [PubMed: 21220692]
15. Yokota A, et al. GM-CSF and IL-4 synergistically trigger dendritic cells to acquire retinoic acid-producing capacity. *Int. Immunol.* 2009 dxp003.
16. Hammerschmidt SI, et al. Retinoic acid induces homing of protective T and B cells to the gut after subcutaneous immunization in mice. *The Journal of clinical investigation.* 2011; 121:3051–3061. [PubMed: 21737878]
17. Villablanca, Mora. MyD88 and Retinoic Acid Signaling Pathways Interact to Modulate Gastrointestinal Activities of Dendritic Cells. *Gastroenterology.* 2011
18. Bhat PV. Retinal dehydrogenase gene expression in stomach and small intestine of rats during postnatal development and in vitamin A deficiency. *FEBS letters.* 1998; 426:260–262. [PubMed: 9599020]
19. Frota-Ruchon A, Marcinkiewicz M, Bhat PV. Localization of retinal dehydrogenase type 1 in the stomach and intestine. *Cell Tissue Res.* 2000; 302:397–400. [PubMed: 11151452]
20. Wagner M, Han B, Jessell TM. Regional differences in retinoid release from embryonic neural tissue detected by an in vitro reporter assay. *Development.* 1992; 116:55–66. [PubMed: 1483395]
21. Kane MA, Folias AE, Napoli JL. HPLC/UV quantitation of retinal, retinol, and retinyl esters in serum and tissues. *Anal Biochem.* 2008; 378:71–79. [PubMed: 18410739]

22. Greter M, H J, Chow A, Hashimoto D, Mortha A, Agudo-Cantero j, Bogunovic M, Gautier EL, Miller J, Merad M. GM-CSF Controls Nonlymphoid Tissue Dendritic Cell Homeostasis but Is Dispensable for the Differentiation of Inflammatory Dendritic Cells. *Immunity*. 2012
23. Mueller S, Germain R. Stromal cell contributions to the homeostasis and functionality of the immune system. *Nature reviews. Immunology*. 2009; 9:618–629.
24. Roozendaal R, Mebius R. Stromal Cell-Immune Cell Interactions. *Annual Review of Immunology*. 2011; 29:23–43.
25. Hammerschmidt S, et al. Stromal mesenteric lymph node cells are essential for the generation of gut-homing T cells in vivo. *J. Exp. Med*. 2008
26. Molenaar R, et al. Lymph Node Stromal Cells Support Dendritic Cell-Induced Gut-Homing of T Cells. *J Immunol*. 2009; 183:6395–6402. [PubMed: 19841174]
27. Iliev ID, Mileti E, Matteoli G, Chieppa M, Rescigno M. Intestinal epithelial cells promote colitis-protective regulatory T-cell differentiation through dendritic cell conditioning. *Mucosal immunology*. 2009; 2:340–350. [PubMed: 19387433]
28. Wang S, et al. MyD88-Dependent TLR1/2 Signals Educate Dendritic Cells with Gut-Specific Imprinting Properties. *The Journal of Immunology*. 2011; 187:141–150. [PubMed: 21646294]
29. Agace. IRF4 Transcription-Factor-Dependent CD103+CD11b+ Dendritic Cells Drive Mucosal T Helper 17 Cell Differentiation. *Immunity*. 2013
30. van de Laar L, Coffey PJ, Woltman AM. Regulation of dendritic cell development by GM-CSF: molecular control and implications for immune homeostasis and therapy. *Blood*. 2012; 119:3383–3393. [PubMed: 22323450]
31. Wagner MA. Use of reporter cells to study endogenous retinoid sources in embryonic tissues. *Methods Enzymol*. 1997; 282:98–107. [PubMed: 9330280]

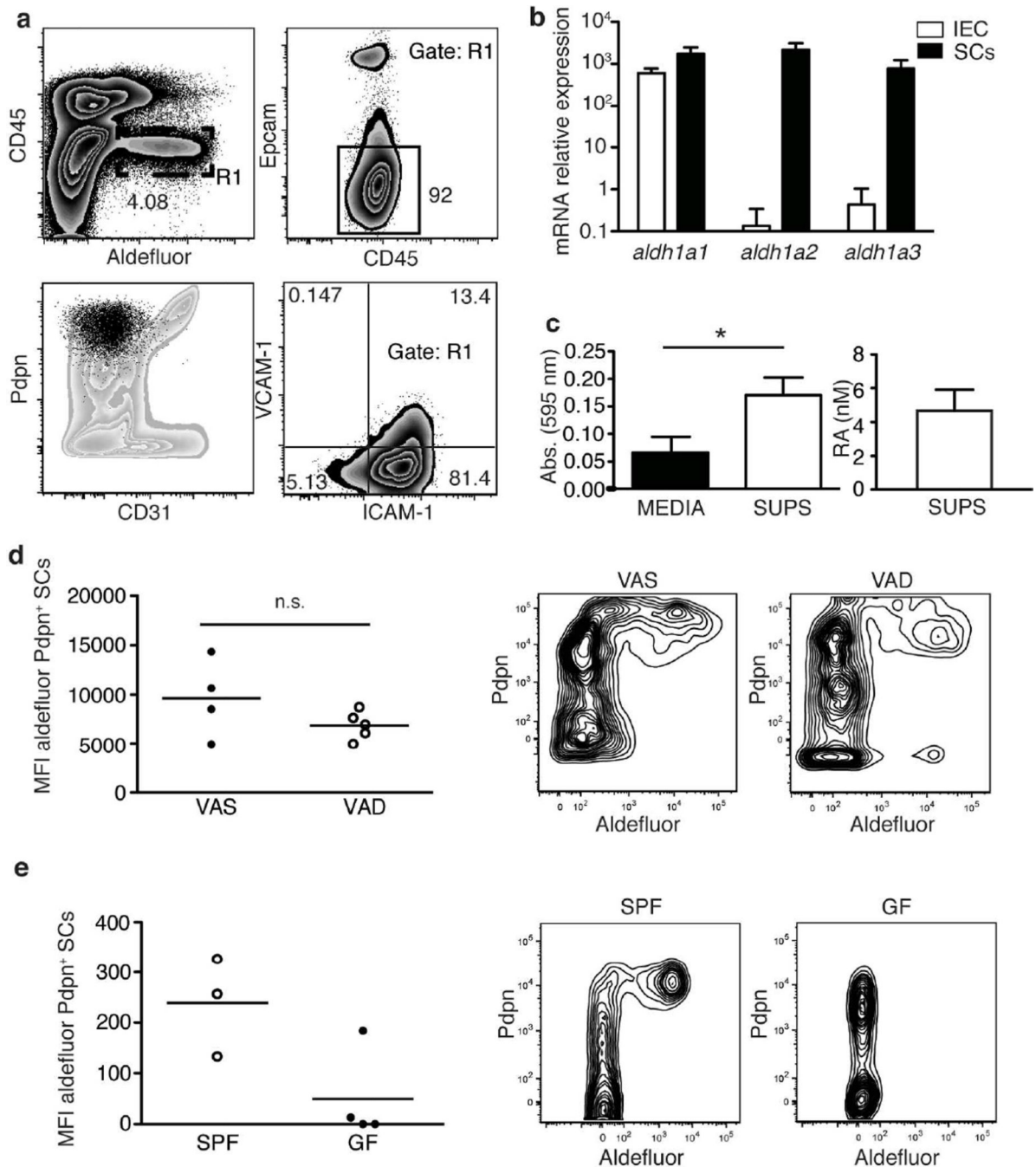


Figure 1. A subset of LP SCs have the capacity to produce RA

a Analysis of RALDH activity using aldefluor in single-cell suspensions prepared from SI LP and assessed by flow cytometry for the indicated markers. Left lower panel displays CD45⁻aldefluor⁺ cells (gate R1, black color) within the whole SI LP SC population (grey color). Data shows a representative experiment of more than 5 independent experiments.

b mRNA levels of the RA producing enzymes RALDH1 (*aldh1a1*) RALDH2 (*aldh1a2*) and RALDH3 (*aldh1a3*) were measured by qRT-PCR in sorted CD45⁻Epcam⁻CD31⁻Pdpn⁺

cells (SCs, black bars) and CD45⁻Epcam^{hi} cells (IEC, white bars). Data shown correspond with RNA from three independent experiments that were quantified at the same time.

c Supernatants from sorted SCs were used to stimulate F9-RARE-lacZ cells and β galactosidase production by these cells measured using a colorimetric reaction. Left panel compares the absorbances obtained when F9-RARE-lacZ cells were left untreated (black bar) or supernatants were added to the culture (white bar), right panel shows an estimation of the RA cc present in the supernatants. Represented is the average \pm s.d. from three independent experiments pooled together ($p=0.0269$ *t*-test non paired).

d Aldefluor staining of CD45⁻ Pdpn⁺ stromal cells was compared between specific pathogen free (SPF) and germ free mice (GF) or **e** between vitamin A sufficient (VAS) and vitamin A (VAD) mice. Shown is a representative experiment out of three independent experiments ($p = 0.18$ n.s. *t*-test non paired).

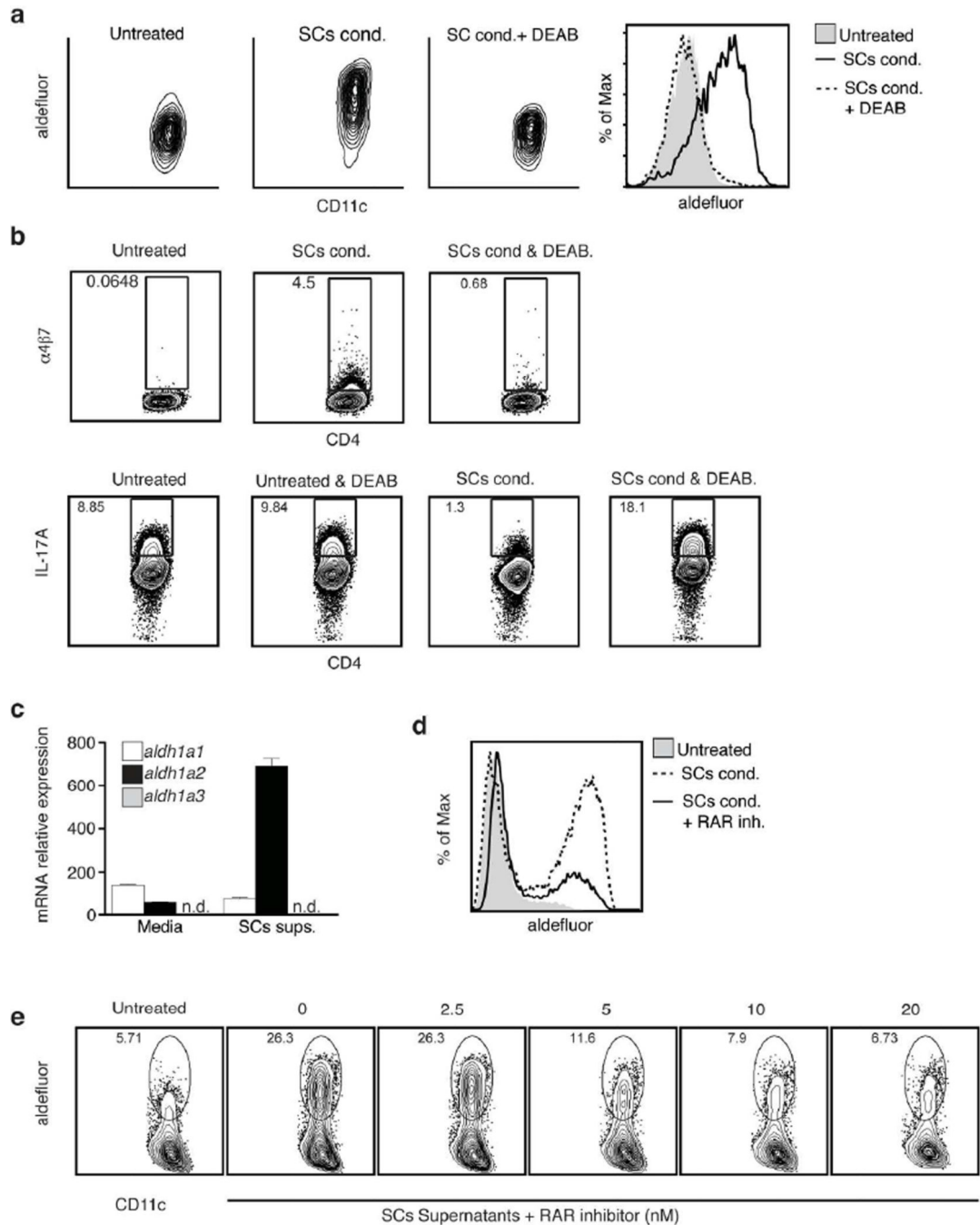


Figure 2. Aldefluor positive SCs are abundant within the intestinal lamina propria and locate closely to intestinal DCs

a–c Confocal imaging of aldefluor stained live SI explants after IEC removal. Aldefluor staining was followed by immunofluorescence with the indicated antibodies, anti-CD31 (a), anti-CD11c (b) or anti-CD11c plus anti-podoplanin (b, right panel) or plus anti-CD103 (c, right panel). In the indicated images (b, central panel) explants were stained with aldefluor in the presence of the RALDH inhibitor DEAB. White arrowheads point out aldefluor⁺ DCs in close contact with aldefluor⁺ SCs, yellow arrowheads indicate podoplanin⁺ aldefluor⁺

cells. Quantification shows the percentage of CD11c⁺ CD103⁺ cells in direct contact with aldefluor bright LP cells from more than ten different images.

Author Manuscript

Author Manuscript

Author Manuscript

Author Manuscript

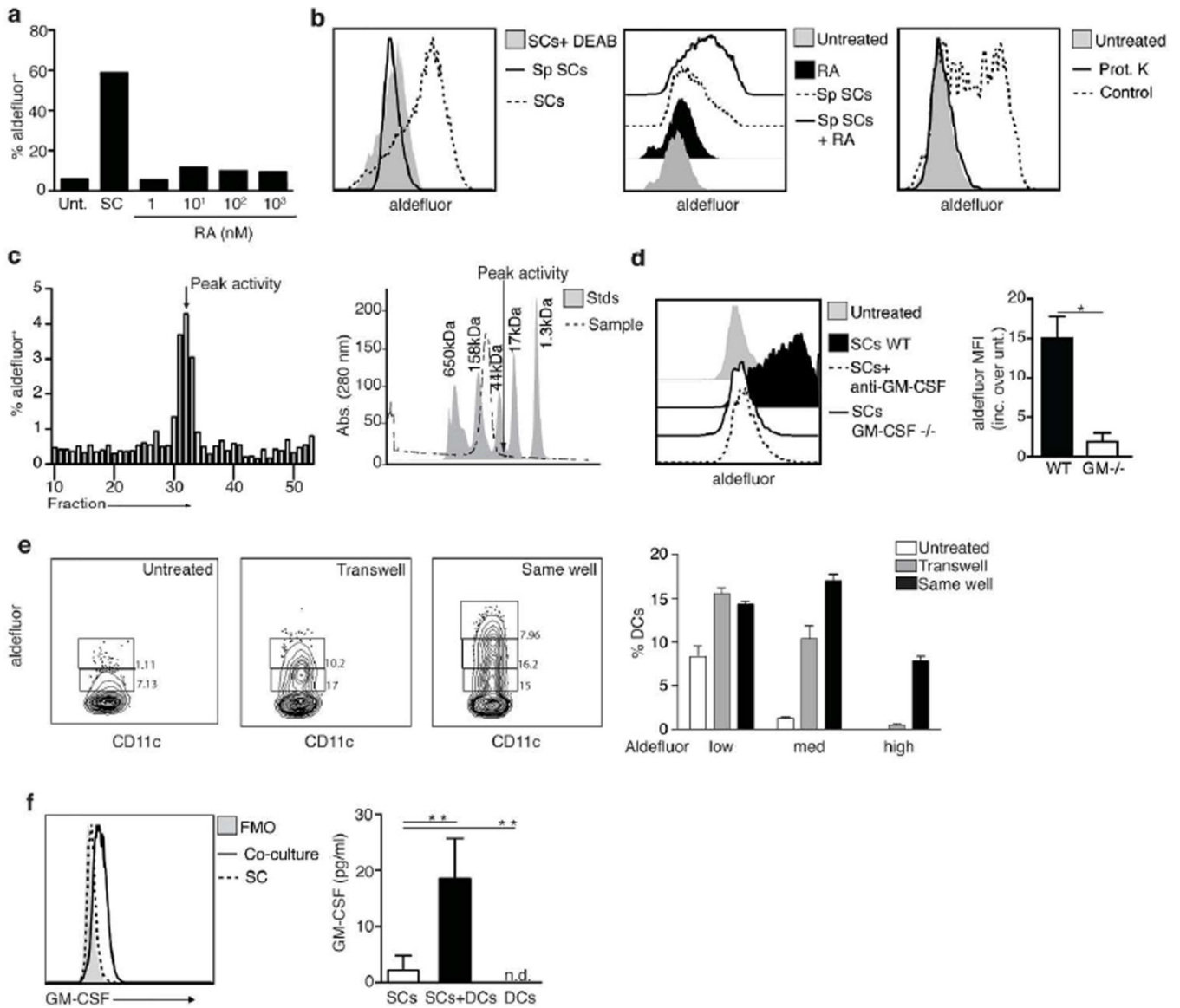


Figure 3. DCs require RAR signaling to induce RA producing enzymes when cultured with Pdpn⁺ CD31⁻ SI LP SCs

a Aldefluor staining of splenic DCs (gated CD45⁺MHCII^{hi}CD11c⁺) after 24h culture alone (Untreated) or together with SI SCs (SCs cond.). DEAB (100 μM) was added at the time of the staining together with aldefluor where indicated. Data show one representative experiment of more than 5 experiments with identical results.

b FACs analysis of IL-17A (left panel) or α4β7(right panel) in PMA/Ionomycin re-stimulated OTII cells primed with splenic DCs for 4–5 days. When indicated, DEAB (10 μM) was added to the DC-T cell culture and maintained during the whole length of the experiment. Analysis shows the result from one representative experiment of at least two experiments with similar results.

c mRNA levels of the RA producing enzymes RALDH1 (*aldh1a1*) RALDH2 (*aldh1a2*) and RALDH3 (*aldh1a3*) were measured by qRT-PCR in splenic DCs after 24hr culture in media alone or media supplemented with SC supernatants (SCs sups, obtained as in Fig1a). Data

shown correspond to RNA from three independent experiments that were quantified at the same time.

d Aldefluor staining of splenic DCs (gated CD45⁺MHCII^{hi}CD11c⁺) after 24h culture alone or together with sorted SCs (SCs cond, left panel) or their supernatants (SCs sups, right panel). The global RAR global antagonist BMS204493 (RAR inh) was added to the culture at concentration of 20nM or otherwise indicated. Data shown are from one representative experiment of at least three experiments.

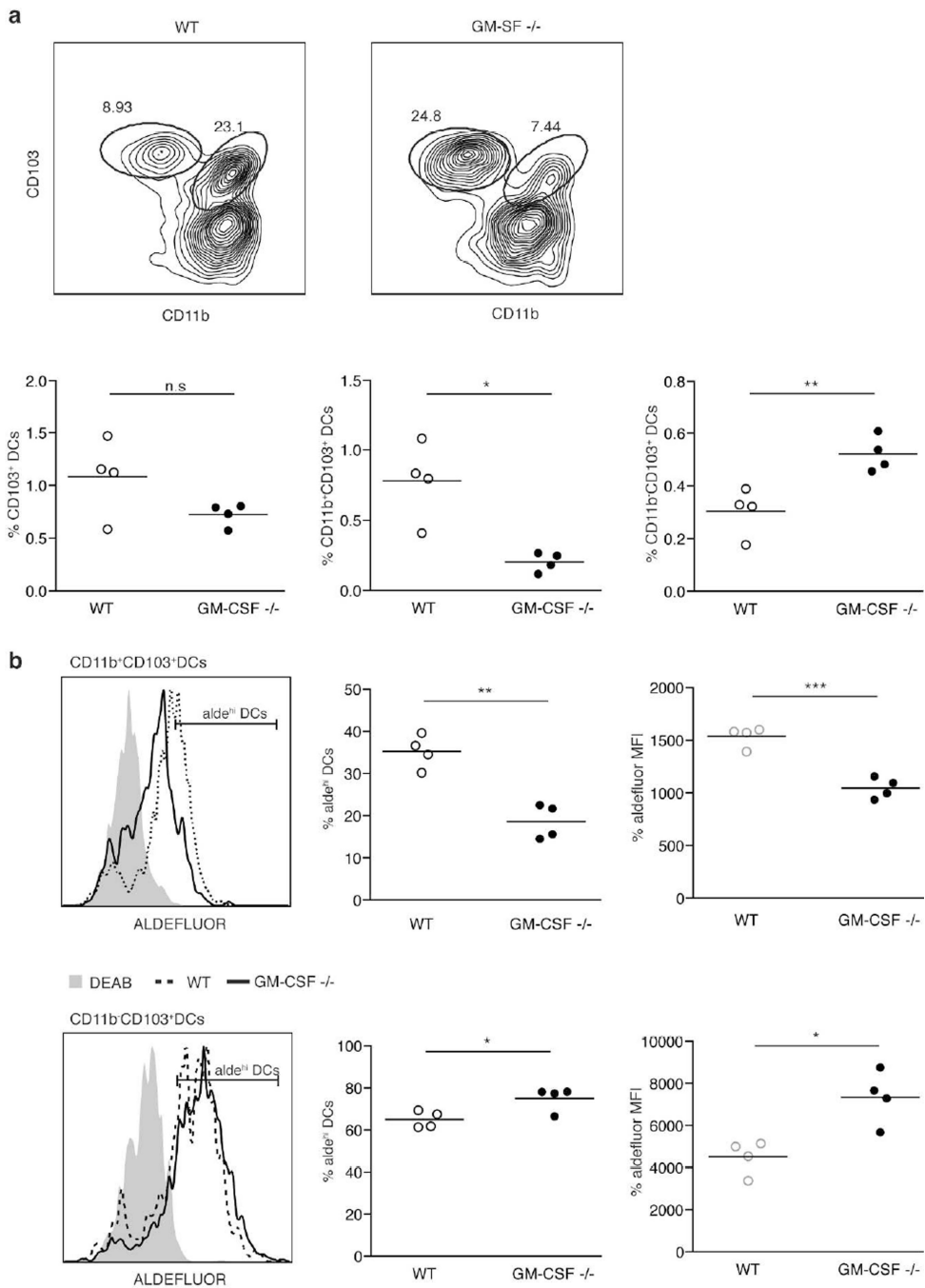


Figure 4. GM-CSF production by stromal cells is enhanced by DCs and required for the imprinting of DCs with high RALDH activity

a Aldefluor staining of splenic DCs after 24 h treatment with SI LP

CD45⁻Epcam⁻Pdpn⁺CD31⁻ stromal cells (SCs) or with media supplemented with increasing concentrations of RA. Data from one representative experiment of three experiments with similar results

b Left panel shows aldefluor staining of a cell line established from sorted primary CD45⁻Pdpn^{hi} splenic cells (Sp SCs) versus SI LP CD45⁻Epcam⁻Pdpn⁺CD31⁻ stromal cells

(SCs). Middle panel shows aldefluor staining of splenic DCs (CD45⁺CD11c⁺MHCII^{hi} gate) cultured for 24h with the aforementioned cell line in the presence or not of RA (100 nM). Right panel shows aldefluor staining of splenic DCs treated with RA plus concentrated sups from the aforementioned cell line. Sups were digested with proteinase K when indicated. Shown is the data from one representative experiment of two.

c left panel shows aldefluor staining of splenic DCs after 24h treatment with RA plus sequential fractions of the sups from Sp SCs (fractionation details within the material and methods section). Right panel shows an estimate of the size of the proteins contained within the fraction that gave us the most activity.

d left panel shows aldefluor staining of splenic DCs cultured for 24 hours alone or together with SCs from WT or GM-CSF KO mice. Anti-GM-CSF blocking antibody was added where indicated. Right panel shows the fold increase on aldefluor staining (mean fluorescence intensity, MFI) on splenic DCs co-cultured with SI LP

CD45⁻Epcam⁻Pdpn⁺CD31⁻ stromal cells (SCs) from WT vs GM-CSF KO mice. Data shows the results from three independent experiments * P < 0.05 (unpaired *t*-test)

e Aldefluor staining of splenic DCs after 24h culture with SI LP CD45⁻Epcam⁻Pdpn⁺CD31⁻ stromal cells (SCs) in the same well or separated by a permeable membrane (transwell) Bar graphs shows data from three replicate wells within one experiment. Data shows one representative experiment out of two.

f shows GM-CSF by intracellular staining (left panel) or ELISA (right) on SI LP CD45⁻Epcam⁻Pdpn⁺CD31⁻ stromal cells (SCs) cultured for 24h alone or together with splenic DCs. Left panel shows one representative experiment out of three. Right panel shows data analyzed corresponding to five independent experiments ** P < 0.01 (unpaired *t*-test)

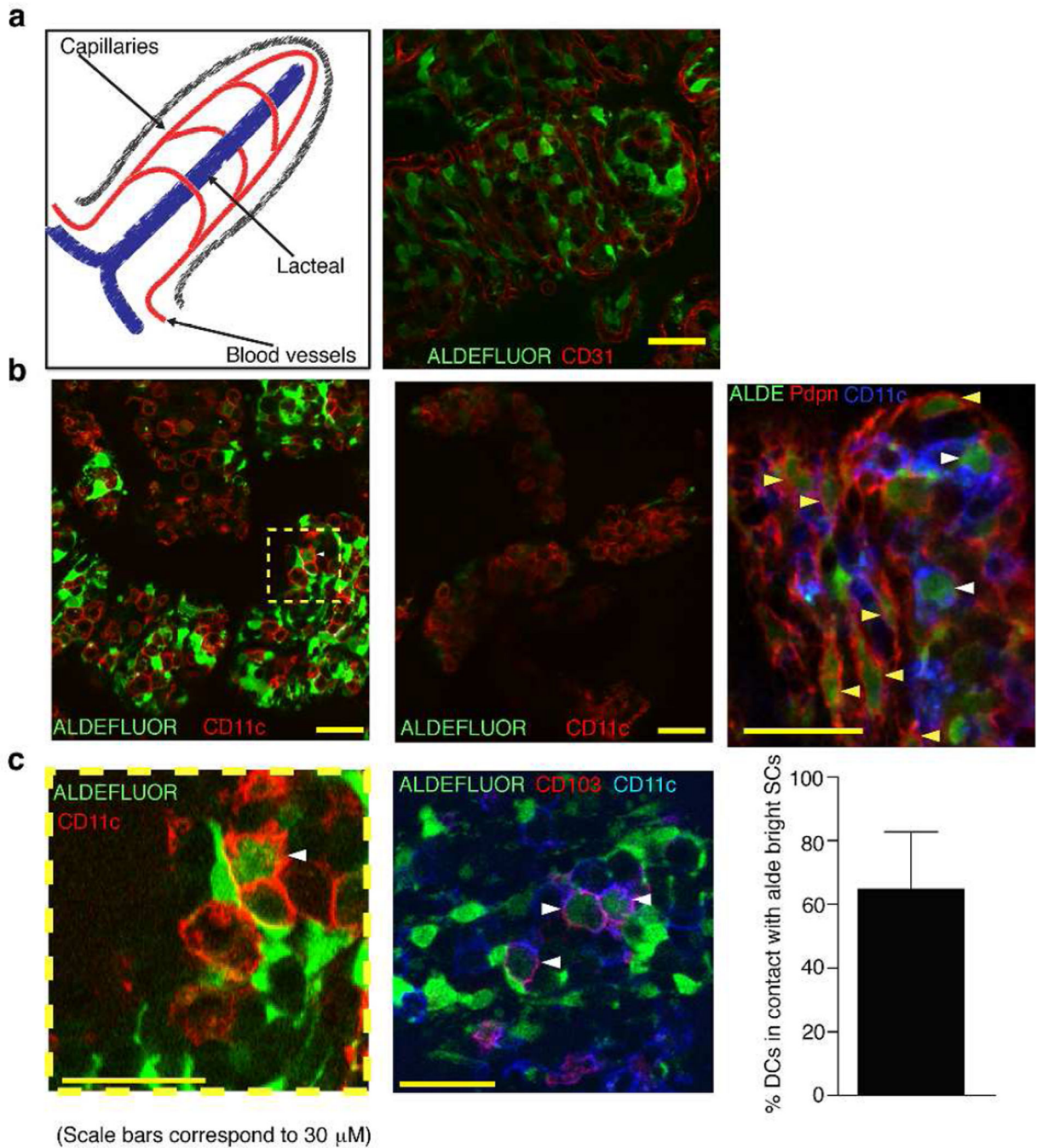


Figure 5. CD11b⁺CD103⁺ DC numbers and RA producing capacity are diminished in GM-CSF^{-/-} mice

a Upper row shows CD11b vs CD103 staining of SI LP DCs (gated as CD45⁺ CD11c^{hi} MHCII^{high}) in WT vs GM-CSF KO mice. Lower row shows the percentage of the indicated populations among the total number of SI LP cells in WT vs GM-CSF KO mice, left panel total CD103⁺ DCs, middle panel CD11b⁺CD103⁺ DCs and right panel CD11b⁻CD103⁺ DCs.

b Aldefluor staining of the CD11b⁺ (upper row) and CD11b⁻ (lower row) SI LP CD103⁺ DC population in WT vs GM-CSF KO mice indicating the percentage of aldefluor high cells (middle panel) as well as the aldefluor mean fluorescence intensity (MFI) for the whole population (right panel).

Data shows one representative experiment of more than three performed (n.s. P>0.05, * P<0.05, ** P<0.001, *** P<0.0005)

Author Manuscript

Author Manuscript

Author Manuscript

Author Manuscript